Role of neutron transfer in sub-barrier fusion

Rudra N. Sahoo,[1,*] Malika Kaushik,[1] Arshiya Sood,[1] Arzoo Sharma,[1] Swati Thakur,[1] Pawan Kumar,[1] Md. Moin Shaikh,[2] Rohan Biswas,[3] Abhishek Yadav,[4] Manoj K. Sharma,[5] J. Gehlot,[3] S. Nath,[3] N. Madhavan,[3] R. G. Pillay,[1] E. M. Kozulin,[6] G. N. Knyazheva,[6] K. V. Novikov,[6] and Pushpendra P. Singh[1,†]

[1]*Department of Physics, Indian Institute of Technology Ropar, Rupnagar 140 001, Punjab, India*
[2]*Variable Energy Cyclotron Centre, 1/AF, Bidhannagar, Kolkata 700 064, India*
[3]*Nuclear Physics Group, Inter-University Accelerator Centre, New Delhi 110 067, India*
[4]*Department of Physics, Jamia Millia Islamia, New Delhi 110 025, India*
[5]*Department of Physics, S. V. College, Aligarh 202 001, Uttar Pradesh, India*
[6]*Flerov Laboratory of Nuclear Reactions, Joint Institute for Nuclear Research, Dubna, Russia*

(Received 22 April 2019; revised 4 November 2019; accepted 29 July 2020; published 13 August 2020)

The fusion excitation function of ^{35}Cl + ^{130}Te system has been measured in a wide energy range, i.e., $E_{\text{c.m.}} = 94$–121.6 MeV, from sub-barrier to above-barrier energies and compared with the ^{37}Cl + ^{130}Te system to investigate the role of neutron transfer channels in sub-barrier fusion cross-section enhancement. In comparison, the reduced fusion excitation function of ^{35}Cl + ^{130}Te system shows a significant enhancement over the ^{37}Cl + ^{130}Te system at sub-barrier energies. This enhancement is correlated with the presence of six positive Q-value neutron transfer channels in the ^{35}Cl + ^{130}Te system compared to none in the ^{37}Cl + ^{130}Te system. Aiming to probe how fusion at sub-barrier energies responds to different coupling schemes, the excitation functions of both the systems have been analyzed in the framework of the coupled-channels approach on the same footing. The results and coupled-channels analysis presented in this work hints towards the importance of neutron transfer channels in sub-barrier fusion in addition to the inclusion of inelastic excitations of interacting partners. The findings of this work are discussed in light of the conclusions presented by Kohley *et al.* [Phys. Rev. Lett. **107**, 202701 (2011)], in which the role of positive Q-value neutron transfer channels in sub-barrier fusion was studied.

DOI: 10.1103/PhysRevC.102.024615

I. INTRODUCTION

Sub-barrier fusion in heavy-ion induced reactions offers possibilities to explore static and dynamic properties of nuclei and to investigate the advancement of tunneling phenomena in terms of couplings of inelastic excitations and transfer channels [1–7]. Further, the understanding of sub-barrier fusion leads to comprehensive knowledge of suitable conditions for the synthesis and exploration of superheavy elements, sources of energy in astrophysical objects, lower breakup threshold of weakly bound nuclei, and fusion reaction dynamics at extreme low energies [8–14]. Generally, the fusion of two heavy nuclei occurs if the entrance channel can overcome the effective barrier formed due to the cumulative effect of repulsive Coulomb and attractive nuclear potential. However, fusion at sub-barrier energies has been experimentally ascertained in different reports [12,15–17], and showed substantial enhancement over the standard one-dimensional barrier penetration model (1-d BPM) [18]. In numerous existing studies, the sub-barrier fusion has been attributed to quantum tunneling [16,19], static deformations, dynamic deformations leading to the coupling of inelastic excitations [15,17,20], and the onset of transfer channels [4,21].

Beckerman *et al.* first observed the role of positive Q-value neutron transfer channels in sub-barrier fusion in ^{58}Ni + ^{58}Ni, ^{64}Ni + ^{64}Ni, and ^{58}Ni + ^{64}Ni systems [22]. The excitation functions of the former two systems at sub-barrier energies have been found to be identical within the experimental uncertainties. For the ^{58}Ni + ^{64}Ni system, the excitation function showed large enhancement as compared to the former two systems. Albeit all intrinsic properties of these systems are the same, the presence of a positive Q-value $+2n$ transfer channel in the ^{58}Ni + ^{64}Ni system is an exception which has been correlated with sub-barrier fusion enhancement. Subsequently, the presence of neutron transfer channels with positive Q value in ^{16,18}O + ^{60,58}Ni, ^{28}Si + ^{90,94}Zr [23], ^{32}S + ^{58,64}Ni, ^{90,94,96}Zr [24–26], and ^{40,48}Ca + ^{124,132}Sn, ^{90,96}Zr [27–29] systems was correlated with the sub-barrier fusion enhancement. However, the positive Q-value neutron transfer channels show no influence in sub-barrier fusion in ^{130}Te + ^{58,64}Ni [30], ^{60,64}Ni + ^{100}Mo [31], ^{132}Sn + ^{58}Ni [30] and ^{64}Ni + ^{118}Sn [32], ^{16,18}O + ^{76,74}Ge, ^{92}Mo, ^{118}Sn [33–35], and ^{40}Ar + ^{112,122}Sn [36] systems. Further, for ^{40}Ar + ^{144,148,154}Sm [36], ^{46,50}Ti + ^{124}Sn [37], ^{32,36}S + ^{110}Pd [38], and ^{40,48}Ca + ^{48}Ca [39] systems, the sub-barrier fusion enhancement has been interpreted by considering a combined effect of neutron transfer channels with positive Q values and

*rnsahoo@iitrpr.ac.in
†pps@iitrpr.ac.in

deformations. The ambiguity in the aforementioned observations suggests that the coupling of neutron transfer channels may not be sufficient but is of high importance to describe the sub-barrier fusion enhancement [40,41].

Several dynamical models have been proposed to interpret the sub-barrier fusion dynamics. In the coupled-channels approach, Hagino *et al.* [20] included the coupling of the positive Q-value $+2n$ transfer channel to explain the enhancement of sub-barrier fusion. Zagrebaev *et al.* [8,42] formulated a model by incorporating neutron transfer channels and used the semiclassical approximation for transfer probability. Sargsyan *et al.* [43] applied the quantum diffusion approach to analyze fusion excitation functions of ^{11}Be + ^{209}Bi and ^{15}C + ^{232}Th reactions. A phenomenological model was given by Rowley *et al.* [44] by imposing transfer channels on coupled-channels calculations. Stelson *et al.* [24] emphasized that the fusion occurs due to neutron flow during the process of interaction. Esbensen *et al.* numerically calculated sub-barrier fusion cross sections of a few systems by including dynamical deformations in the coupled-channels calculations [45]. It has been found that the coupled-channels calculations do not reproduce the cross sections of some systems, particularly because of probable transfer channels. The coupling of neutron transfer has been included in the calculations to interpret sub-barrier fusion [46,47]. Pollarolo and Winther proposed a semiclassical approximation to explain the experimental fusion cross-sections [48], which suggests that the transfer probability is quite small as compared to large projectile energy dissipation. Apart from these models, the universal fusion function [21] and the Wolski energy scaling law [49] have been proposed to interpret sub-barrier fusion data. Despite the existing experimental and theoretical studies, the role of different couplings in the behavior of sub-barrier fusion is not yet fully concluded and thus continues to be an active area of investigations.

In the present work, the role of different couplings in sub-barrier fusion is explored. The fusion excitation function of the ^{35}Cl + ^{130}Te system is measured in a wide energy range around the Coulomb barrier energies, and compared with that obtained for ^{37}Cl + ^{130}Te systems [50] to probe the role of transfer channels with positive Q value in sub-barrier fusion. The comparison of these systems is particularly interesting because the ^{35}Cl + ^{130}Te system has six positive Q-value neutron transfer channels compared to none in ^{37}Cl + ^{130}Te systems. The Q-value data of neutron transfer channels for these systems are given in Table II. The excitation functions of both the systems have been analyzed in the framework of the coupled-channels approach using CCFULL code [20] on the same footing, and the findings of the present work are discussed in light of the conclusions drawn in Ref. [30] for ^{58,64}Ni + ^{130}Te systems. The experimental setup and data reduction procedures are discussed in Sec. II of this paper. Section III deals with the results and interpretation, and Sec. IV summarizes the findings of the present work.

II. EXPERIMENTAL AND DATA REDUCTION PROCEDURES

The experiments were performed at the Inter-University Accelerator Centre, New Delhi, by employing a recoil mass separator, the Heavy Ion Reaction Analyser (HIRA) [51]. The setup and methodology are detailed in Ref. [50]. However, a brief account of experimental conditions that are unique to this work is presented here for ready reference. The target ^{130}Te of thickness ≈200 μg/cm^2, fabricated on a carbon backing of 20 μg/cm^2 using ultrahigh vacuum evaporation technique [52], is bombarded by ^{35}Cl beams of energies $E_{\text{c.m.}} = 94 - 121.6$ MeV, i.e., from 10% below to 15 % above the Bass barrier $V_B = 105.14$ MeV. A ^{130}Te target was mounted in beam facing the carbon foil configuration inside the target chamber of HIRA maintained at a 10^{-6} mbar vacuum. Two silicon surface barrier detectors each having 1 mm diameter aperture were mounted at 9.8 cm distance from the beam interaction point on the target foil subtending an angle of ±15.5° on either side of the beam direction to monitor the beam. The evaporation residues (ERs) were detected at the focal plane of HIRA through a multiwire proportional counter of an active area of 150×50 mm^2. The acceptance of HIRA was kept at 5 msr, 2.2° polar angle, and the transmission efficiency of the spectrometer was determined using the semimicroscopic Monte Carlo code TERS [53].

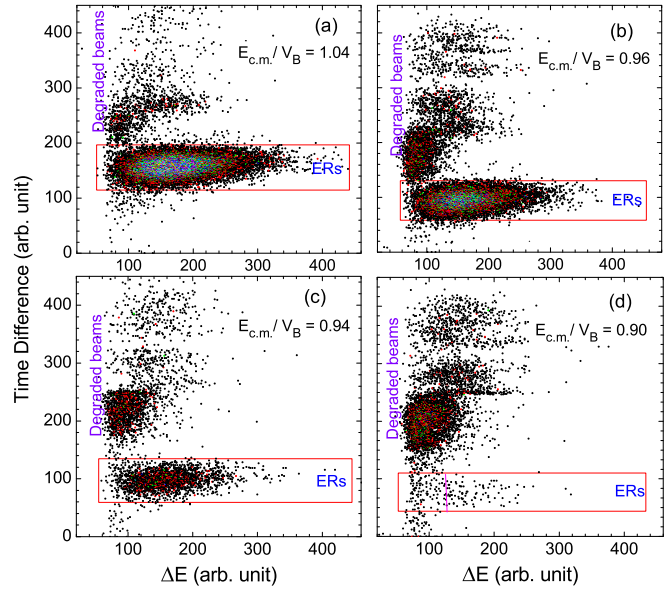

FIG. 1. ΔE-time spectra obtained for the ^{35}Cl + ^{130}Te system at incident energies $E_{\text{c.m.}}/V_B = 0.90$, 0.94, 0.96, and 1.04.

In the present work, pulsed beams with a repetition rate of 2 μs were used to achieve a clear separation between ERs and degraded beams. The time interval between two successive pulses was estimated to be greater than the flight time of ERs (i.e., approximately 1.5 μs at the energy around the barrier) during the passage through the dispersive elements of HIRA. The ERs were identified by making an electronic gate between time of flight (ToF) and corresponding energy loss (ΔE) through the multiwire proportional counter. As a representative case, a few ΔE-time spectra are shown in Fig. 1 in which the ERs are well separated from the beamlike particles. However, at lowest measured energy, i.e., $E_{\text{c.m.}}/V_B = 0.90$, the ERs are not very well separated from the degraded beamlike particles, particularly below the channel number 125 on the x

TABLE I. Experimentally measured fusion cross sections (σ_{fus}) in the $^{35}Cl + ^{130}Te$ system at different energies ($E_{c.m.} = 94.0 - 121.6$ MeV).

$E_{c.m.}$ (MeV)	σ_{fus} (mb)	$E_{c.m.}$ (MeV)	σ_{fus} (mb)
94.0	0.034 ± 0.010	106.7	174 ± 21
95.6	0.243 ± 0.045	108.2	225 ± 26
97.2	1.37 ± 0.17	109.8	286 ± 33
98.8	4.5 ± 0.6	112.2	397 ± 46
100.3	15.6 ± 1.8	114.5	466 ± 60
101.9	40.2 ± 4.5	116.9	548 ± 70
103.5	71 ± 8	119.3	598 ± 72
105.0	111 ± 13	121.6	659 ± 83

axis, that is marked by a vertical pink line within the specified gate. To estimate the accurate number of ERs in the region, the number of events in this region was estimated between these two areas by comparing with the ratio of events at higher energies where the ERs are separated from degraded beamlike particles. The fusion cross sections at different energies were calculated using a standard formulation [50].

III. RESULTS AND INTERPRETATIONS

Experimentally measured fusion cross sections at different energies are given in Table I, and plotted in Fig. 2 as a function of $E_{c.m.}$. It may be pointed out that the cross sections presented in Table I are almost entirely due to fusion-evaporation, as the fission contribution in the $^{35}Cl + ^{130}Te$ system is found to be negligible by the theoretical model code PACE4 [54]. The uncertainties quoted in the fusion cross sections are absolute errors consisting of the statistical error and the error due to transmission efficiency of the recoil mass separator.

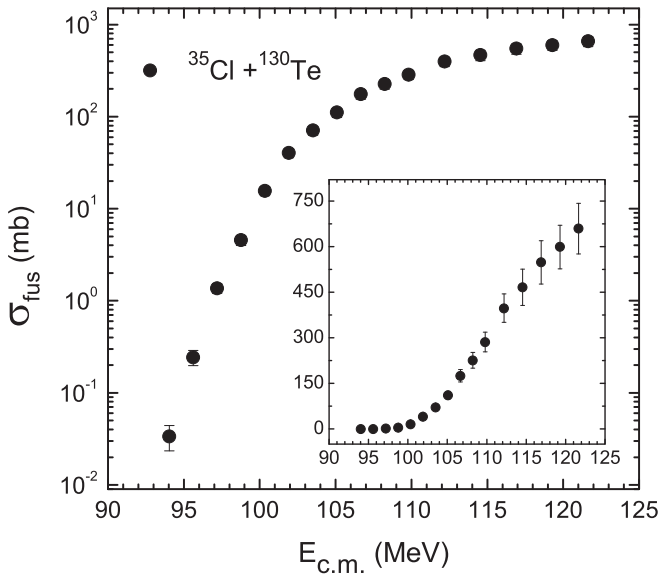

FIG. 2. Experimentally measured fusion excitation function of the $^{35}Cl + ^{130}Te$ system. The inset shows the cross sections on a linear scale for better visualisation of errors at above-barrier energies.

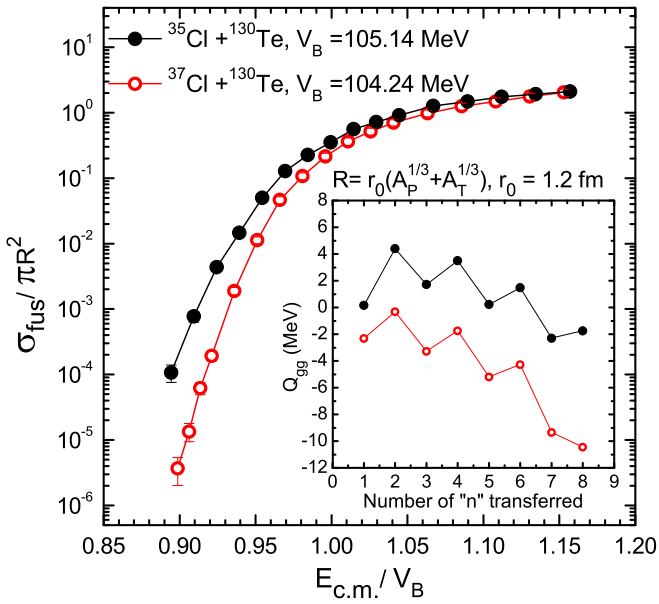

FIG. 3. Experimentally measured reduced fusion excitation functions of $^{35}Cl + ^{130}Te$ (present work) and $^{37}Cl + ^{130}Te$ [50] systems. The inset shows Q values of neutrons transfer channels for both systems. Lines and curves are to guide the eyes.

A. Role of neutron transfer in sub-barrier fusion

In heavy-ion induced reactions, the transfer of nucleons between interacting partners is regulated by optimum Q value (Q_{opt}). Based on the value of Q_{opt}, the onset of all transfer channels is hindered, including neutron stripping, but not the neutron pickup and proton stripping [55]. Among these transfer processes, the neutron pickup is more probable as compared to the proton stripping, because neutrons are insensitive to the Coulomb barrier. For neutron transfer channels, the charge of the projectile and target remains the same, corresponfing to zero optimum Q value ($Q_{opt} = 0$). Therefore, in the present work, the ground state Q value (Q_{gg}) is taken into account for the interpretation of fusion cross sections.

In order to investigate the role of neutron transfer channels in sub-barrier fusion enhancement, reduced fusion excitation functions of $^{35}Cl + ^{130}Te$ (present work) and $^{37}Cl + ^{130}Te$ [50] systems are compared in Fig. 3. It may be pointed out that the comparison of $^{35,37}Cl + ^{130}Te$ systems should be made on the same footing. Therefore, the center-of-mass beam energies ($E_{c.m.}$) and fusion cross sections (σ_{fus}) are scaled with the respective Bass barriers (V_{Bass}) and geometrical cross sections (πR^2) to remove the effects of barrier position and nuclear radius of the two systems in comparison. As can be seen from Fig. 3, the reduced fusion excitation function of the $^{35}Cl + ^{130}Te$ system is found to be substantially higher than that of the $^{37}Cl + ^{130}Te$ system in the sub-barrier energy region, indicating a strong influence of projectile structure on sub-barrier fusion as the target is same for both the systems. From the geometric point of view, the fusion cross sections in the $^{37}Cl + ^{130}Te$ system at different energies are expected to be higher than in the $^{35}Cl + ^{130}Te$ system. Since the fusion cross sections for both the systems are corrected by the normalization procedure mentioned above, the reduced fusion

TABLE II. The g.s. → g.s. Q values of neutron transfer channels in $^{35,37}\mathrm{Cl} + {}^{130}\mathrm{Te}$ systems.

System	$+1n$	$+2n$	$+3n$	$+4n$	$+5n$	$+6n$
$^{35}\mathrm{Cl} + {}^{130}\mathrm{Te}$	+0.61	+4.38	+1.71	+3.49	+0.21	+1.46
$^{37}\mathrm{Cl} + {}^{130}\mathrm{Te}$	−2.31	−0.32	−3.27	−1.74	−5.18	−4.26

excitation functions presented in Fig. 3 should not display any significant difference within the experimental uncertainties. The enhancement of the fusion excitation function in the case of the $^{35}\mathrm{Cl} + {}^{130}\mathrm{Te}$ system over the $^{37}\mathrm{Cl} + {}^{130}\mathrm{Te}$ system points toward the static properties of the projectile, and evolution of dynamic properties at the time of interaction of projectile and target nuclei. The sub-barrier fusion enhancement in the case of the $^{35}\mathrm{Cl} + {}^{130}\mathrm{Te}$ system may be attributed to the combined effect of positive Q-value neutron transfer channels, the valence shell neutrons, and static deformation.

However, it is interesting to note that the $^{35}\mathrm{Cl} + {}^{130}\mathrm{Te}$ system has six positive Q-value neutron transfer channels as compared to none in the $^{37}\mathrm{Cl} + {}^{130}\mathrm{Te}$ system (refer to Table II), which may be primarily responsible for the sub-barrier fusion enhancement. Further, it may be pointed out that in $^{35}\mathrm{Cl}$, the outermost shell, i.e., $1d_{3/2}$, is half filled whereas the outermost shell is fully filled in $^{37}\mathrm{Cl}$.

To attain stability, $^{35}\mathrm{Cl}$ needs two additional neutrons in its outermost shell. During the interaction of $^{35}\mathrm{Cl}$ and $^{130}\mathrm{Te}$, neutrons may flow in either direction due to the configuration mixing between the interacting partners. Since the process of neutron transfer is regulated by the ground state Q value of the reaction, neutron flow takes place from $^{130}\mathrm{Te}$ to $^{35}\mathrm{Cl}$ due to the positive ground state Q value. During the process of neutron exchange, sometimes a strong neck is formed between the interacting partners, leading to the complete fusion of projectile and target nuclei. Based on this qualitative picture, it may be inferred that the $^{35}\mathrm{Cl}$ projectile shows larger fusion probability as compared to the $^{37}\mathrm{Cl}$ projectile with the $^{130}\mathrm{Te}$ nucleus. This argument is in line with the Stelson neutron flow model [56], but inconsistent with the observation that the heaviest isotopes of each element, which have the smallest neutron binding energies, give the largest fusion cross sections in the near-barrier region [57]. Moreover, both $^{35}\mathrm{Cl}$ and $^{37}\mathrm{Cl}$ projectiles are deformed in different configurations, with $\beta_2 \approx -0.24$ and $\approx +0.11$, respectively, and the excited states of the projectiles are nearly of the same order of magnitude [58,59]. The oblate shape of the $^{35}\mathrm{Cl}$ projectile may reduce the effective barrier for fusion as compared to the $^{37}\mathrm{Cl}$ projectile, leading to the enhanced fusion cross section for $^{35}\mathrm{Cl} + {}^{130}\mathrm{Te}$ system in the sub-barrier region.

Further, it is difficult to emphasize the exact reason for sub-barrier fusion enhancement in case of the $^{35}\mathrm{Cl} + {}^{130}\mathrm{Te}$ system over the $^{37}\mathrm{Cl} + {}^{130}\mathrm{Te}$ system just by looking at the comparison of excitation functions, whether the enhancement is only due to individual effects of projectile deformation and neutron transfer channels or the combined effect of both. The fusion excitation functions of both the systems have been analyzed in the framework of the coupled-channels approach using CCFULL code on the same footing to realize the prime cause of sub-barrier fusion enhancement. This code solves the coupled-channels equations to compute the complete fusion cross section and mean angular momenta of the compound nucleus by taking into account the couplings to all orders and does not introduce the expansion of the coupling potential. It may be pointed out that this code has been developed for even-even systems. However, in some cases [60,61], a modified version of this code [62] was employed successfully to interpret fusion excitation functions.

B. Analysis with coupled-channels code CCFULL

In order to interpret the behavior of sub-barrier fusion in the $^{35}\mathrm{Cl} + {}^{130}\mathrm{Te}$ system, the fusion excitation function has been analyzed using coupled-channels code CCFULL. The excitation functions of both systems presented in Fig. 3 have been treated on the same footing to establish the parametrization for coupled-channels analysis. For these calculations, suitable nuclear potential parameters have been chosen by following the standard Woods Saxon parametrization and fitting the cross sections at above-barrier energies as per the one-dimensional barrier penetration model (1-d BPM) because the effect of static and dynamic properties becomes negligible at above-barrier energies in the process of complete fusion [20,62,63]. The nuclear potential parameters $V_0 = 75.6$ MeV, $r_0 = 1.2$ fm, and $a_0 = 0.72$ fm are chosen for $^{37}\mathrm{Cl} + {}^{130}\mathrm{Te}$ system. As a test case, the coupled-channels calculations for the $^{37}\mathrm{Cl} + {}^{130}\mathrm{Te}$ system are presented in Fig. 4(a). As is evident from this figure, the coupled-channels calculations with the couplings of in-elastic excitations of the projectile and target nuclei provide a satisfactory description of the experimentally measured excitation function for the entire measured energy range [50]. On similar footing, the coupled-channels calculations have been performed for the $^{35}\mathrm{Cl} + {}^{130}\mathrm{Te}$ system, in which the nuclear potential parameters $V_0 = 79.40$ MeV, $r_0 = 1.2$ fm, and $a_0 = 0.72$ fm have been used [62,63]. The outcome of these calculations is plotted in Fig. 4(b) along with the experimentally measured fusion excitation function. As shown in this figure, the coupled-channels calculations underpredict the fusion excitation function of $^{35}\mathrm{Cl} + {}^{130}\mathrm{Te}$ system in the sub-barrier energy region even though all low-lying inelastic excitations are included in the calculations by following the same procedure as in the $^{37}\mathrm{Cl} + {}^{130}\mathrm{Te}$ system. Thus, the sub-barrier fusion enhancement over the coupled-channels calculations may be an indication of some physical effect which is not included in the coupled-channels calculations.

Further, from the comparison of $^{35,37}\mathrm{Cl} + {}^{130}\mathrm{Te}$ systems presented in Fig. 3, the sub-barrier fusion enhancement may be correlated with the presence of six positive Q-value neutron transfer channels in the $^{35}\mathrm{Cl} + {}^{130}\mathrm{Te}$ system. In order to investigate whether or not the sub-barrier fusion enhancement may be explained in terms of neutron transfer channels, coupled-channels analysis has been performed by including the couplings of the neutron transfer channel. The Q-value profile of neutron transfer channels for both of these systems is given in the inset of Fig. 3. In coupled-channels calculations, the inclusion of transfer coupling requires a transfer form factor (F_{tr}) derived from the experimentally measured transfer

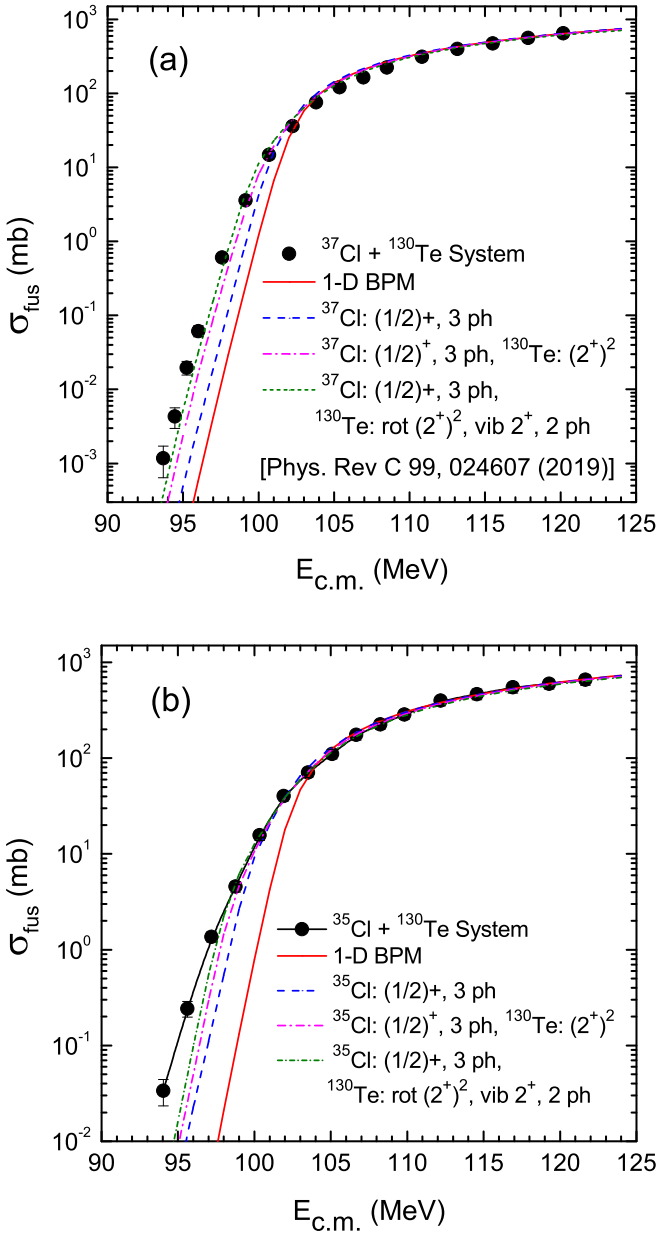

FIG. 4. The measured fusion excitation function of (a) the ^{37}Cl + ^{130}Te system [50] and (b) the ^{35}Cl + ^{130}Te system. The coupled-channels calculations—performed by including the couplings of inelastic excitations of interacting partners, i.e., the $(1/2)^{+}$ state of the projectile and the $(2^{+})^{2}$ and vibrational 2^{+} (two-phonon) state of the target by taking into account $\beta 2 = 0.11$—are displayed. Lines and curves are self-explanatory.

probability. Since the transfer cross sections have not been measured in the present work, the coupled-channels calculations are performed with different values of transfer form factors, ranging from 0.2 to 0.5 MeV. As a representative case, the outcome of coupled-channels calculations with $+2n$ transfer coupling for the values of transfer form factor $F_{tr} =$ 0.2 and 0.3 is plotted in Fig. 5. As can be seen in this figure, with an increase in transfer form factor from 0.2 to 0.3 MeV, the coupled-channels calculations provide an improved description of experimentally measured fusion cross sections at sub-barrier energies, but considerably under-predict at above-barrier energies. Similar observations were reported in Refs. [64,65]. Therefore, to fit the excitation functions, the calculations have been performed with a larger diffuseness parameter, 0.74 fm instead of 0.72 fm, and using a transfer form factor $F_{tr} = 0.3$ MeV. This combination reproduces fusion cross sections fairly well in the sub-barrier energy region within the experimental uncertainties, but underpredicts at above-barrier energies. Based on this analysis, it can be inferred that the simultaneous description of fusion crosssections from sub-barrier to above-barrier energy is not observed for any combination of input parameters in coupled-channels calculations. However, the positive Q-value neutron transfer channels should be taken into account while interpreting the sub-barrier fusion enhancement. For further clarification on the role of neutron transfer channels in sub-barrier fusion enhancement, the inclusive measurement of fusion and differential transfer measurements are in order and should be performed.

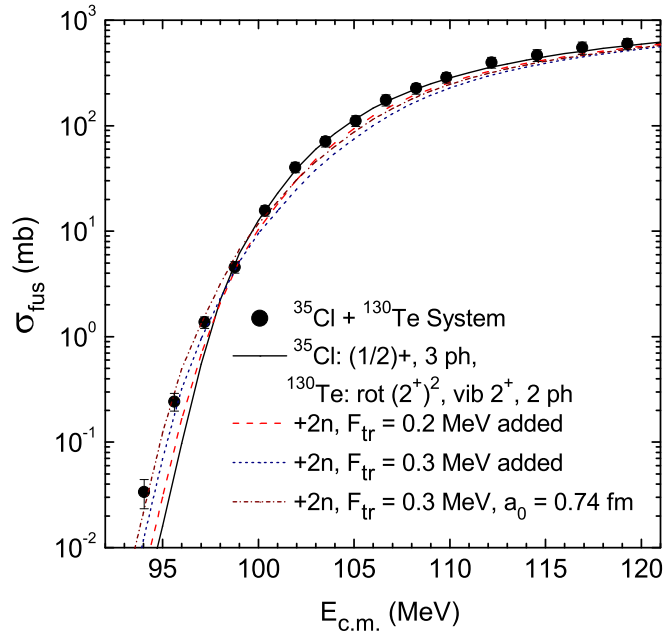

FIG. 5. Experimentally measured fusion excitation function of the ^{35}Cl + ^{130}Te system compared with the outcome of coupled-channels calculations performed by including $+2n$ transfer coupling for different transfer form factors, i.e., $F_{tr} = 0.2$ and 0.3 MeV. The lines and symbols are self-explanatory.

C. Comparison of ^{35,37}Cl + ^{130}Te and ^{58,64}Ni + ^{130}Te systems

Recently, Kohley *et al.* [30] reported that the presence of positive Q-value neutron transfer channels has very little, if any, influence on sub-barrier fusion. In Ref. [30], the reduced fusion excitation functions of ^{58,64}Ni + ^{130}Te systems were found to be equivalent even though the ^{58}Ni + ^{130}Te system has 11 positive Q-value neutron transfer channels in comparison to only one in the ^{64}Ni + ^{130}Te system. It has been found that the Te + Ni fusion measurements show lack of transfer effects. However, for ^{35,37}Cl + ^{130}Te systems, a

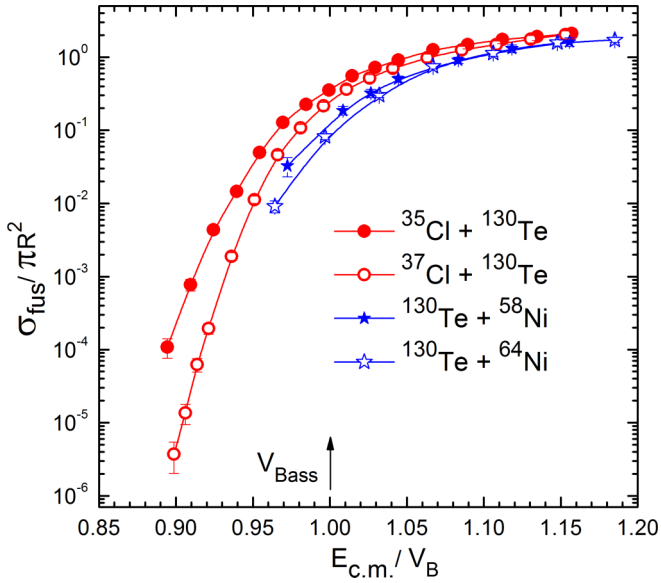

FIG. 6. Comparison of reduced fusion excitation functions of ^{130}Te + ^{58,64}Ni [30], ^{35}Cl + ^{130}Te [50], and ^{37}Cl + ^{130}Te (present work) systems.

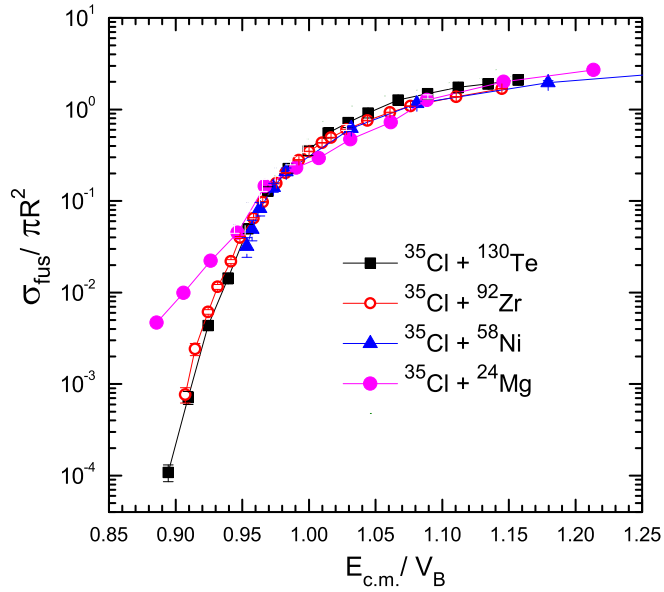

FIG. 7. Comparison of reduced fusion excitation functions of ^{35}Cl + ^{130}Te, ^{92}Zr, ^{58}Ni, and ^{24}Mg systems. The excitation functions of all the systems fall on the same line except for ^{35}Cl + ^{24}Mg systems.

correlation between positive Q-value neutron transfer channels and sub-barrier fusion has been noticed. Figure 6 shows reduced excitation functions of ^{58,64}Ni + ^{130}Te [30] systems in comparison with ^{35,37}Cl + ^{130}Te systems. As can be seen from this figure, the fusion cross sections for ^{58,64}Ni + ^{130}Te systems were measured down to energies $3-4\%$ below the barrier, while in the present work the fusion measurements are extended down to an energy 10% below the barrier. The reduced fusion excitation functions of ^{58,64}Ni + ^{130}Te [30] and ^{35,37}Cl + ^{130}Te systems display almost identical behavior down to the energies 3-4% below the barrier. However, the splitting of excitation functions in the case of ^{35,37}Cl + ^{130}Te systems is found to be more prominent at lower energies in a range from 4% to 10% below the barrier, suggesting the role of positive Q-value neutron transfer channels on sub-barrier fusion. It would be interesting to investigate ^{58,64}Ni + ^{130}Te [30] systems down to the deep sub-barrier energies to conclude the role of positive Q-value neutron transfer channels for ^{58,64}Ni + ^{130}Te [30] systems.

D. Target systematics with ^{35}Cl projectile

Existing data for ^{35}Cl + X systems have been reanalysed and compared with the ^{35}Cl + ^{130}Te system in Fig. 7. The fusion cross sections (σ_{fus}) are normalized with the geometrical cross section (πR^2), and the bombarding energies ($E_{c.m.}$) are normalized with the Bass barrier height (V_B) to incorporate the effect of the nuclear radius and barrier of different systems in comparison. As can be noticed from the figure, for this comparison, the ^{35}Cl + ^{130}Te, ^{35}Cl + ^{92}Zr [66], ^{35}Cl + ^{58}Ni [67], and ^{35}Cl + ^{24}Mg [68] systems are chosen to have same projectile on targets of increasing mass. In all cases, the fusion cross sections were measured well below the barrier energies. However, for the ^{35}Cl + ^{130}Te system (present work), the measurement of cross sections is extended one order of magnitude down as compared to the other systems. It may be noted that the reduced fusion excitation functions of ^{35}Cl + ^{130}Te, ^{35}Cl + ^{92}Zr, and ^{35}Cl + ^{58}Ni systems follow the same trend in the sub-barrier energy region, but for the ^{35}Cl + ^{24}Mg system the excitation function is visibly enhanced as compared to other systems at sub-barrier energies. This enhancement may be due to the positive Q value (Q_{fus}) of the fusion reaction ^{35}Cl + ^{24}Mg. For ready reference, the values of Q_{fus} for these reactions are given in Table III. As can be seen from this table, only the ^{35}Cl + ^{24}Mg system has positive Q_{fus}. Therefore, it can be inferred that the sub-barrier fusion is also sensitive to the fusion Q value.

IV. SUMMARY AND CONCLUSIONS

In the present work, the fusion excitation function of the ^{35}Cl + ^{130}Te system has been measured at energies from 10% below to 15% above the Coulomb barrier, and compared with the ^{37}Cl + ^{130}Te [50] system. It has been found that the reduced fusion excitation function of the ^{35}Cl + ^{130}Te system shows a substantial enhancement over the ^{37}Cl + ^{130}Te system in the sub-barrier energy region, which has been analyzed in view of the presence of positive Q-value neutron transfer

TABLE III. The N/Z of ^{130}Te, ^{92}Zr, ^{58}Ni, and ^{24}Mg, and fusion Q values (Q_{fus}) of these targets with ^{35}Cl projectile.

System	N/Z (target)	Q_{fus} (MeV)	Reference
^{35}Cl + ^{130}Te	1.50	−53.43	present work
^{35}Cl + ^{92}Zr	1.30	−39.57	[66]
^{35}Cl + ^{58}Ni	1.07	−20.23	[67]
^{35}Cl + ^{24}Mg	1.00	+13.41	[68]

channels in the $^{35}Cl + ^{130}Te$ system. The coupled-channels analysis has been performed for both systems on the same footing. The coupled-channels analysis hints towards the role of neutron transfer channels, especially $+2n$ transfer, and inelastic excitations couplings in sub-barrier fusion. The findings of the present work have been discussed in light of the results presented by Kohley *et al.* [30] for $^{58,64}Ni + ^{130}Te$ systems. Further, the excitation function of the $^{35}Cl + ^{130}Te$ system has been compared with the results of other measurements in which ^{35}Cl has been used as a projectile. Based on this comparison, it has been inferred that the reaction Q value also plays an important role in the enhancement of fusion cross section at sub-barrier energies.

Additionally, the qualitative signature of the valence shell effect has been discussed in the present work, and is found to be consistent with the neutron flow model. Based on the results and analysis presented here, it may be concluded that the sub-barrier fusion cross sections are enhanced due to the superposition of tunneling and the couplings of inelastic excitations and positive Q-value reaction channels. It would be interesting to extend such measurements at deep sub-barrier energies for better insights into the role of deformation, nuclear structure, and transfer channel couplings for different systems. It may, however, be pointed out that a deeper understanding of sub-barrier fusion dynamics requires the identification of the contribution of the individual input parameters and the channel-by-channel cross-section measurement of transfer events [55,69].

ACKNOWLEDGMENTS

The authors are thankful to the accelerator division of the Inter-University Accelerator Center, New Delhi for their efforts in delivering high quality ^{35}Cl beams, and the target laboratory personnel for their help during the target fabrication. We are pleased to acknowledge R. Chary and Vandana Nanal for valuable discussions during the preparation of this paper. R.N.S gratefully acknowledges support from a Director's Fellowship from the Indian Institute of Technology Ropar, P.P.S. acknowledges the Science and Engineering Research Board, India for an Indo-Russia Project grant, Ref. No. DST/INT/RUS/RSF/P-23, and E. M. Kozulin thanks the Russian Science Foundation for a project grant, Ref. No. 19-42-02014/RSF-DST/2018.

[1] B. B. Back, H. Esbensen, C. L. Jiang, and K. E. Rehm, Rev. Mod. Phys. **86**, 317 (2014), and the references therein.
[2] A. M. Stefanini *et al.*, Phys. Rev. Lett. **74**, 864 (1995); Phys. Rev. C **96**, 014603 (2017).
[3] A. Lemasson *et al.*, Phys. Rev. Lett. **103**, 232701 (2009).
[4] M. Dasgupta, D. J. Hinde, A. Diaz-Torres, B. Bouriquet, C. I. Low, G. J. Milburn, and J. O. Newton, Phys. Rev. Lett. **99**, 192701 (2007).
[5] C. L. Jiang *et al.*, Phys. Rev. Lett. **113**, 022701 (2014), and the references therein.
[6] G. Montagnoli *et al.*, Phys. Rev. C **97**, 024610 (2018)
[7] G. Colucci *et al.*, Phys. Rev. C **97**, 044613 (2018).
[8] V. I. Zagrebaev, V. V. Samarin, and W. Greiner, Phys. Rev. C **75**, 035809 (2007).
[9] W. Loveland, Phys. Rev. C **76**, 014612 (2007).
[10] L. F. Canto *et al.*, J. Phys. G **36**, 015109 (2009); Phys. Rep. **424**, 1 (2006).
[11] M. S. Smith and K. E. Rehm, Annu. Rev. Nucl. Part. Sci. **48**, 401 (1998).
[12] C. L. Jiang, K. E. Rehm, B. B. Back, and R. V. F. Janssens, Phys. Rev. C **75**, 015803 (2007); Phys. Rev. Lett. **89**, 052701 (2002).
[13] Md. Moin Shaikh *et al.*, J. Phys. G **45**, 095103 (2018).
[14] C. L. Jiang *et al.*, Phys. Rev. Lett. **93**, 012701 (2004).
[15] R. G. Stokstad, Y. Eisen, S. Kaplanis, D. Pelte, U. Smilansky, and I. Tserruya, Phys. Rev. Lett. **41**, 465 (1978); Phys. Rev. C **21**, 2427 (1980); **23**, 281 (1981).
[16] C. Y. Wong, Phys. Lett. B **42**, 186 (1972); Phys. Rev. Lett. **31**, 766 (1973).
[17] A. M. Stefanini, L. Corradi, A. M. Vinodkumar, Y. Feng, F. Scarlassara, G. Montagnoli, S. Beghini, and M. Bisogno, Phys. Rev. C **62**, 014601 (2000); A. M. Stefanini, M. Trotta, L. Corradi, A. M. Vinodkumar, F. Scarlassara, G. Montagnoli, and S. Beghini, *ibid.* **65**, 034609 (2002).
[18] J. F. Liang *et al.*, Phys. Rev. Lett. **91**, 152701 (2003), and the references therein.
[19] L. C. Vaz *et al.*, Phys. Rev. C **10**, 464 (1974); L. C. Vaz and J. M. Alexander, *ibid.* **18**, 2152 (1978).
[20] K. Hagino, N. Rowley, and A. T. Kruppa, Comput. Phys. Commun. **123**, 143 (1999).
[21] V. V. Sargsyan, G. G. Adamian, N. V. Antonenko, W. Scheid, and H. Q. Zhang, Phys. Rev. C **85**, 024616 (2012); **85**, 069903(E) (2012); **91**, 014613 (2015).
[22] M. Beckerman *et al.*, Phys. Rev. Lett. **45**, 1472 (1980).
[23] S. Kalkal *et al.*, Phys. Rev. C **81**, 044610 (2010).
[24] P. H. Stelson, H. J. Kim, M. Beckerman, D. Shapira, and R. L. Robinson, Phys. Rev. C **41**, 1584 (1990).
[25] H. M. Jia *et al.*, Phys. Rev. C **89**, 064605 (2014).
[26] H. Q. Zhang *et al.*, Phys. Rev. C **82**, 054609 (2010).
[27] J. J. Kolata *et al.*, Phys. Rev. C **85**, 054603 (2012).
[28] H. Timmers *et al.*, Nucl. Phys. A **633**, 421 (1998).
[29] A. M. Stefanini *et al.*, Phys. Rev. C **73**, 034606 (2006).
[30] Z. Kohley *et al.*, Phys. Rev. Lett. **107**, 202701 (2011).
[31] A. M. Stefanini *et al.*, Eur. Phys. J. A **49**, 63 (2013).
[32] K. T. Lesko, W. Henning, K. E. Rehm, G. Rosner, J. P. Schiffer, G. S. F. Stephans, B. Zeidman, and W. S. Freeman, Phys. Rev. C **34**, 2155 (1986).
[33] C. J. Lin *et al.*, EPJ Web Conf. **66**, 03055 (2014).
[34] M. Benjellom *et al.*, Nucl. Phys. A **560**, 715 (1993).
[35] P. Jacobs *et al.*, Phys. Lett. B **175**, 271 (1986).
[36] W. Reisdorf *et al.*, Nucl. Phys. A **438**, 212 (1985).
[37] J. F. Liang *et al.*, Phys. Rev. C **94**, 024616 (2016), and the references therein.
[38] A. M. Stefanini, D. Ackermann, L. Corradi, J. H. He, G. Montagnoli, S. Beghini, F. Scarlassara, and G. F. Segato, Phys. Rev. C **52**, R1727(R) (1995).
[39] M. Trotta, A. M. Stefanini, L. Corradi, A. Gadea, F. Scarlassara, S. Beghini, and G. Montagnoli, Phys. Rev. C **65**, 011601(R) (2001)

[40] V. A. Rachkov, A. V. Karpov, A. S. Denikin, and V. I. Zagrebaev, Phys. Rev. C **90**, 014614 (2014).
[41] G. L. Zhang, X. X. Liu, and C. J. Lin, Phys. Rev. C **89**, 054602 (2014).
[42] V. I. Zagrebaev, Phys. Rev. C **64**, 034606 (2001).
[43] V. V. Sargsyan *et al.*, Eur. Phys. J. A **49**, 54 (2013)
[44] N. Rowlay *et al.*, Phys. Lett. B **282**, 276 (1992).
[45] H. Esbensen, J.-Q. Wu, and G. F. Bertsch, Nucl. Phys. A **411**, 275 (1983).
[46] H. Esbensen and S. Landowne, Nucl. Phys. A **492**, 473 (1989).
[47] H. Esbensen, C. L. Jiang, and K. E. Rehm, Phys. Rev. C **57**, 2401 (1998).
[48] G. Pollarolo and A. Winther, Phys. Rev C **62**, 054611 (2000).
[49] R. Wolski, Phys. Rev. C **88**, 041603(R) (2013).
[50] Rudra N. Sahoo *et al.*, Phys. Rev. C **99**, 024607 (2019), and the references therein.
[51] A. K. Sinha *et al.*, Nucl. Instrum. Methods Phys. Res. Sect. A **339**, 543 (1994).
[52] R. N. Sahoo *et al.*, Nucl. Instrum. Methods A **935**, 103 (2019).
[53] S. Nath, Comput. Phys. Commun. **180**, 2392 (2009).
[54] A. Gavron, Phys. Rev. C **21**, 230 (1980); LISE++, http://lise.nscl.msu.edu/5_13/lise_5_13.html
[55] L. Corradi, G. Pollarolo, and S. Szilner, J. Phys. G: Nucl. Part. Phys. **36**, 113101 (2009).
[56] P. H. Stelson, Phys. Lett. B **205**, 190 (1988).
[57] P. H. Stelson, in *International Symposium on Heavy-Ion Reaction Dynamics in Tandem Energy Region* (Hitachi, Japan, 1988).
[58] P. Moller, R. Nix, W. D. Mayers, and W. J. Swiatecki, At. Data Nucl. Data Tables **59**, 185 (1995).
[59] https://www.nndc.bnl.gov/nudat2/
[60] M. S. Gautam *et al.*, Nucl. Phys. A **984**, 9 (2019).
[61] G. Colucci *et al.*, Eur. Phys. J. A **55**, 111 (2019), and the references therein.
[62] K. Hagino (private communications).
[63] A. M. Stefanini *et al.*, Phys. Lett. B **679**, 95 (2009).
[64] Khushboo *et al.*, Phys. Rev. C **96**, 014614 (2017).
[65] J. Gao *et al.*, Nucl. Phys. A **929**, 9 (2014).
[66] J. O. Newton, C. R. Morton, M. Dasgupta, J. R. Leigh, J. C. Mein, D. J. Hinde, H. Timmers, and K. Hagino, Phys. Rev. C **64**, 064608 (2001).
[67] W. Scobel, A. Mignerey, M. Blann *et al.*, Phys. Rev. C **11**, 1701 (1975).
[68] Sl. Cavallaro, M. L. Sperduto, B. Delaunay *et al.*, Nucl. Phys. A **513**, 174 (1990).
[69] B. J. Roy, Y. Sawant, P. Patwari, S. Santra, A. Pal, A. Kundu, D. Chattopadhyay, V. Jha, S. K. Pandit, V. V. Parkar, K. Ramachandran, K. Mahata, B. K. Nayak, A. Saxena, S. Kailas, T. N. Nag, R. N. Sahoo, P. P. Singh, and K. Sekizawa, Phys. Rev. C **97**, 034603 (2018).